Biophysical Chemistry 159 (2011) 210–216

Contents lists available at ScienceDirect

Biophysical Chemistry

journal homepage: http://www.elsevier.com/locate/biophyschem

Modulation of allosteric behavior through adjustment of the differential stability of the two interacting domains in E. coli cAMP receptor protein

Jianquan Li [1], J. Ching Lee *

Department of Biochemistry and Molecular Biology, The University of Texas Medical Branch at Galveston, Galveston, Texas 77555–1055

ARTICLE INFO

Article history:
Received 14 April 2011
Received in revised form 23 June 2011
Accepted 24 June 2011
Available online 3 July 2011

Keywords:
Allostery
Protein stability and dynamics
FT-IR
cAMP receptor protein

ABSTRACT

The communication mechanism(s) responsible for the allosteric behavior of E.coli cAMP binding receptor protein, CRP, is still a subject of intense investigation. As a tool to explore the communication mechanism, the mutations at various positions in the cAMP-binding (K52N, D53H, S62F and T127L) or the DNA- binding (H159L) domain or both (K52N/H159L) were generated. The sites and specific nature of side chain substitutions were defined by earlier genetic studies, the results of which show that these mutants have a similar phenotype i.e. they are activated without exogenous cAMP. Presently, no significant changes in the structures of WT and mutant CRPs have been observed. Hence, the pressing issue is to identify a physical parameter that reflects the effects of mutations. In this study, the stability of these various CRP species in the presence of GuHCl was monitored by three spectroscopic techniques, namely, CD, tryptophan fluorescence and FT-IR which could provide data on the stability of α-helices and β-strands separately. Results of this study led to the following conclusions: 1. The α-helices can be grouped into two families with different stabilities. Mutations exert a differential effect on the stability of helices as demonstrated by a biphasic unfolding curve for the helices. 2. Regardless of the locations of mutations, the effects can be communicated to the other domain resulting in a perturbation of the stability of both domains, although the effects are more significantly expressed in the stability of the helices. 3. Although in an earlier study [Gekko, et al. Biochemistry 43 (2004) 3844] we showed that cooperativity of cAMP binding is generally correlated to the global dynamics of the protein and DNA binding affinity, in this study we found that generally there is no clear correlation between functional energetics and stability of secondary structures. Thus, results of this study imply that modulation of allostery in CRP is entropic in nature.

1. Introduction

Biological activities are often regulated by signals transmitted through intra- and inter-macromolecular interactions. A consequence of such signal transmission is the well known phenomenon of allostery. Although the phenomenon has been under intense investigation for many decades, there are still many fundamental questions, such as the pathway of signal transmission in allostery, have yet to be resolved.

We chose the cAMP receptor protein from E.coli, CRP, as a model system to tackle these basic issues. CRP regulates the expression of more than 150 genes by its recognition of specific DNA sequences and subsequent recruitment of RNA polymerase in the presence of cAMP [1–4]. CRP is a homodimeric transcription factor, in which each subunit consists of 209 amino acid residues [5,6]. Each monomer consists of two domains, namely, the cAMP- and the DNA-binding domain shown as green and yellow domain in the monomeric structure of apo-CRP [7–9], respectively, shown in Fig. 1a. The cAMP-binding domain is located in the N-terminal end of the sequence while the DNA-binding domain in the C-terminal. The binding of cAMP in the cAMP-binding domain allosterically increases the binding affinity for specific DNA by the DNA-binding domain, and vice versa [10]. These domains show similarities to domains found in many other proteins from prokaryotes and eukaryotes. The cAMP-binding domain is similar to the regulatory subunit of cAMP-dependent protein kinases and the cyclic nucleotide-binding domain of cyclic nucleotide-gated channels. The DNA binding domain of helix-turn-helix is highly conserved in a large number of DNA-binding proteins [11]. The recently published structures of apo-CRP defined by NMR [9] and crystallography [7] show a significant structural change in comparison to holo-CRP. The change is represented, in general, by a rigid-body rotation of the DNA-binding domain with respect to the cAMP-binding domain [7–9], as shown in Fig. 1b. To understand the communication mechanisms between these two highly utilized domains is of wide significance in biological regulation. A large amount of genetic and *in vitro* studies have focused on mutations that yield a phenotype that does not require exogenous cAMP for activation [12,13]. It was found that most of these

* Corresponding author. Tel.: +1 409 772 2281; fax: +1 409 772 4298.
E-mail address: jclee@utmb.edu (J.C. Lee).
[1] Current address: Discovery Research, Dow AgroSciences LLC, Indianapolis, IN 46268.

0301-4622/$ – see front matter © 2011 Elsevier B.V. All rights reserved.
doi:10.1016/j.bpc.2011.06.015

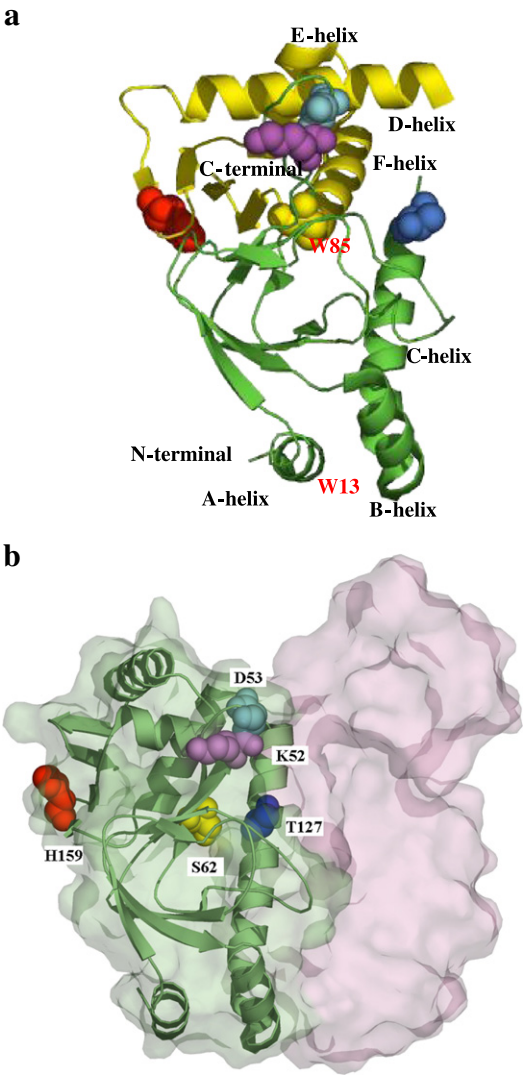

Fig. 1. Structure of CRP. a. Monomeric structure of apo-CRP (PDB 3H1F). The cAMP- and DNA-binding domains are in green and yellow, respectively. The α-helices, the two sequence terminii and locations of the two tryptophan residues are labeled. The mutation sites are identified as colored spheres. The color codes are the same as in Fig. 1b. b. Dimeric structure of holo-CRP (PDB 1G6N). The two subunits are in magenta and green, respectively. The locations of mutation sites are labeled.

sites are not associated with any functional sites for either ligand or DNA binding [13]. The general conclusion indicates that the communications between subunits and domains must be part of the linked reactions that constitute the basic mechanism of allostery in CRP [11]. Employing a series of these mutants identified by genetics, we observed a linear correlation between global protein dynamics and the degree of cooperativity in cAMP binding to CRP [14]. The NMR study on both WT and mutant CRP by Kalodimos and co-workers shows that the major effect of mutations is to affect the dynamics of the protein and domain movement without inducing any significant secondary structural perturbations with the exception of that observed between the C- and D-helix [9]. The conclusion is that the mutations affect the shifting of the conformation distribution between the apo- and holo-conformations [7,9]. Since the effects of mutations seem to be only manifested as a shifting of the distribution of the apo- and holo-states, does that mean that the various mutations, though located in different parts of the protein molecule, perturb the same set of inter-subunit and/or inter-domain structural elements? This study was designed to address this issue by monitoring the effect of mutations on the stability of secondary structural elements.

We chose the following mutations for this study – K52N, D53H, S62F, T127L, H159L and the double mutant of K52N/H159L. The residues and the specific side-chain substitutions are defined by genetic screenings [12,13] and those are the same ones with which we conducted earlier functional studies [14–19]. In CRP, the cAMP-binding domain constitutes residues 1 to 136 and the DNA-binding domain is from residues 139 to 209. Residue 52 resides in β-strand 4 in the cAMP- binding domain and residue 159 resides in β-strand 9 between the D- and E-helix in the DNA-binding domain. An observation of non-additive perturbation to the functions and structures resulted from the mutations at residues 52 and 159 would be an indication of communications between the two domains.

Residues 53 and 62 reside in the cAMP-binding domain. The D53H and S62F mutations yield CRP mutants that exhibit strong positive and negative cooperativity in cAMP binding, respectively. Thus, these mutants are employed to probe the structural properties of mutants with very different degrees of perturbation in cooperativity.

T127 is in the C-helix of the cAMP-binding domain. The T127 residue of the adjacent subunit interacts with the N^6-amino group directly and N^1 of cAMP via a water molecule. The mutation study by Harman and co-workers showed that T127 is important in stabilizing CRP structure and precise repositioning of T127 side chain upon binding cAMP is required for CRP activation [20]. Thus, we wish to elucidate the effect of T127 in transmitting the allosteric signal from the cAMP binding pocket to the DNA-binding domain.

The locations of the mutation sites are shown in Fig. 1a and b. In this study we wish to probe the effects of mutations on the stability of CRP and secondary structural elements in CRP. We monitored the global stability of the protein by CD and fluorescence spectroscopies. We further distinguished the stability of the two classes of secondary structures, namely α-helices and β-strands by FT-IR.

2. Materials and methods

2.1. Materials

The concentration of CRP was determined by the absorption coefficient 40800 M^{-1} cm^{-1} at 278 nm for CRP dimer. The buffer used in all experiments was TEK(100) (50 mM Tris, 1 mM EDTA, 100 mM KCl, pH7.8).

2.2. Circular Dichroism

Circular dichroism measurements were performed by using an Aviv Model 60 DS spectropolarimeter using 4 μM of CRP. CD spectra were measured over the range of 210–270 nm using a 1.0 cm path-length cell. Every spectrum was recorded in 0.5 nm wavelength increments, and the signal was obtained for one second at each wavelength. For every sample, including protein and reference solutions, two repetitive scans were performed and averaged. The fraction f, of folded CRP, was calculated from the equation:

$$f = (\chi - \chi_{unfolded}) / (\chi_{folded} - \chi_{unfolded}) \quad (1)$$

where χ, χ_{folded} and $\chi_{unfolded}$ are the CD or fluorescence signal at any concentration of GuHCl, that of folded and unfolded CRP, respectively. χ_{folded} and $\chi_{unfolded}$ were derived by linear extrapolation of the measured signals at the pre-denaturation and post-denaturation regions using our previously published procedure [21]. The energetics of stability is related to f by:

$$\Delta G = -RT\ln(1-f) / f \quad (2)$$

$$\Delta G = \Delta G^0 - m[GuHCl] \quad (3)$$

where ΔG^0 is the free energy change at 0 M GuHCl; m is the slope of the plot of ΔG vs [GuHCl], the concentration of GuHCl.

2.3. Fluorescence

CRP unfolding by GuHCl was also monitored by intrinsic fluorescence at the excitation and emission wavelengths of 290 and 345 nm, respectively, using a Perkin-Elmer LS50B spectrofluorometer and 4 μM of CRP.

2.4. FT-IR measurements

10 μl aliquots of buffer and CRP at ~50 μM in buffer were separately lyophilized for 2 hours. The dried buffer sample was to provide the background spectrum. Appropriate amount of de-ionized, distilled H_2O and stock GuHCl were added to both dried buffer and CRP to make up solutions of the desired final GuHCl concentrations. The total volume of added H_2O and stock 5.25 M GuHCl in either buffer or CRP sample was 10 μl. Samples were mixed by pippeting and were incubated at 4 °C overnight. Control experiments showed that lyophilization had no considerable effect on the binding affinities of cAMP to CRP and after 2 h of incubation; the area associated with the 2nd derivative has reached its equilibrium with no further change. Thus, an overnight incubation was deemed sufficient for reaching an equilibrium state.

The reference or sample solutions were injected into the CaF_2 cell with the pathlength of about 6 μm. 200 scans of FTIR spectra with a resolution of 4 cm^{-1} were collected in a Single-Beam Bomem MB Series FT-IR Spectrometer (Quebec, Canada). The absorbance spectra for samples and buffer were acquired using the empty cell as references. Then the reference spectra were subtracted from the sample spectra to give the protein spectra by the software PROTA (BOMEM). The FT-IR protein spectra were truncated in the range of 1700 to 1600 cm^{-1}; the second derivative was calculated to enhance resolution. The peak frequency of the second derivative was identical to the original peak frequency. The peak intensity was negative and proportional to the original peak intensity [22]. In CRPs, the peaks for α-helices and β-sheets were at about 1653 and 1633 cm^{-1}, respectively. The areas were obtained by integrating between two valleys of α- or β-peaks separately on the software BOMEM_GRAMS/32 (Version 4.04). All areas were normalized by dividing the areas at 0.0 M of GuHCl.

3. Results

3.1. Denaturation monitored by CD

There are two popular ways to unfold protein, thermal and chemical perturbations. With respect to CRP, thermal unfolding leads to irreversible aggregation under our experimental conditions. However, chemically induced unfolding has proven to be reversible in our earlier study [21].

Circular dichroism was used to monitor the denaturation of WT and six CRP mutants. The CD signal at 222 nm was employed to monitor the secondary structures of CRP at different GuHCl concentrations. The data can best be represented by a two-state process. Fig. 2 shows the unfolding curves of all the CRP samples. The fitted curves were not shown so as to provide a clearer presentation. However, Fig. S1 (Supplementary Material) showed a representation of the fitting to the original data. The concentrations of GuHCl corresponding to the mid-points of the unfolding curves, $C_{1/2}$, and the steepness of transition, as expressed by the m-value, are summarized in Table 1. The unfolding curves of the other CRP mutants show that these mutants exhibit similar $C_{1/2}$ values and the m-values are in general smaller than that of the WT and T127L CRP. The calculated values for ΔG^0 are listed in Table 1. The denaturation study as monitored by CD shows that mutations have an effect on the stability of the protein. In most cases, mutation decreases the stability of CRP.

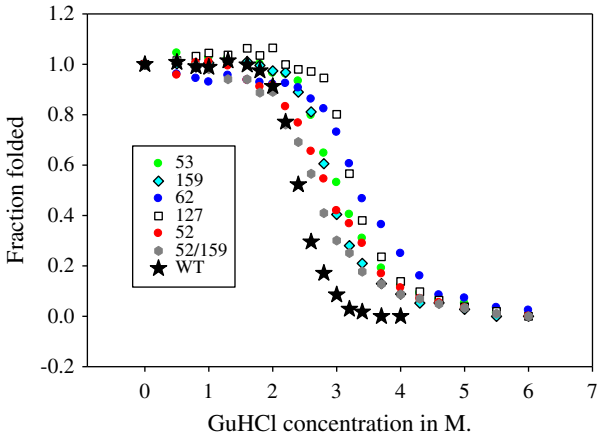

Fig. 2. Chemical denaturation of CRP samples monitored by CD at 222 nm. The symbols and identity of CRP samples are: ●, D53H; ◇, H159L; ●, S62F; □, T127L; ●, K52N; ●, K52N/H159L; ★, WT.

3.2. Denaturation monitored by fluorescence

In order to provide additional information on the unfolding process of CRP and its mutants, we monitored the process by the fluorescence of the tryptophan residues. There are two tryptophan residues in each WT and mutant CRP subunit. Both of them are located in the N-terminal domain which is predominantly populated by β-strands, as shown in Fig. 1a. The two tryptophan residues in CRP are located at position 13 (A-helix) and 85 (β strand 7). 80% of the tryptophan fluorescence is contributed by W13 with approximately 20% of the signal originating from W85 because W85 is buried in CRP [23].

Fig. 3 shows the results of unfolding as monitored by fluorescence. In comparing the results shown in Figs. 2 and 3, it is obvious that the shape of the unfolding curves is dependent on the spectroscopic technique employed. An interesting difference is the m-value associated with the unfolding curves. The m-values are very similar when the unfolding is monitored by fluorescence. These results imply that fluorescence might be sensing the unfolding of an entity that is different from that of CD. Due to the locations of the two tryptophan residues being in the cAMP binding N-terminal domain, the results in Fig. 3 might reflect more of the unfolding of this particular domain while the CD data reflects a more extensive unfolding entity.

3.3. Denaturation monitored by FT-IR

We wish to dissect the unfolding process in greater details to distinguish the stabilities of the secondary structures of α-helices and β-strands. Hence, we developed a procedure to monitor the unfolding process via FT-IR.

3.3.1. Control experiments with myoglobin–

GuHCl was selected as denaturant instead of urea because urea absorbs in the range from 1700 to 1600 cm^{-1} in FT-IR measurements. The absorption peak of GuHCl was at about 1672 cm^{-1}. The second derivative peaks of α-helices and β-strands in CRP appear at about 1654 and 1633 cm^{-1}, respectively. The interference from GuHCl is most likely to affect only the peak of α-helices. Although the buffers with the same GuHCl concentrations were used as references, the exact match of GuHCl absorption between protein samples and corresponding references was very difficult. In order to investigate the extent of interference, myoglobin, which contains only α-helices, was used as a control. At 3.0 M GuHCl, the absorption peak of GuHCl was

Table 1
Summary of unfolding data and function energetics.

Protein	CD			Fluorescence		FT-IR α-helix		FT-IR β-strand		[a]Dimerization	[b]cAMP binding	[a]DNA binding	[c]F_0
	[d]ΔG^0	[e]$C_{1/2}$	[f]m	[e]$C_{1/2}$	[f]m	[e]$C_{1/2}$	[f]m	[e]$C_{1/2}$	[f]m	[d]ΔG	[d]$\Delta\Delta G$	[i]K_a	
WT	7.0	3.0	2.3	2.9	1.6	2.2	0.6	2.9	2.1	11.8	−0.4	49.0	[j]0.27
K52N	3.6	3.1	1.2	2.8	1.2	1.7	0.5	2.8	1.3	8.1	0.9	6.7	0.36
D53H	4.9	3.2	1.6	2.6	1.7	[g]1.1/2.8	[g]0.7/0.3	2.7	1.4	10.9	−1.8	731	0.28
S62F	4.0	3.2	1.3	3.4	1.7	0.9	0.2	3.3	1.6	12.3	1.5	0.54	0.39
T127L	7.3	3.5	2.2	3.0	1.7	2.5	1.1	3.1	2.1	10.5	0.7	0.12	0.28
H159L	5.9	3.1	2.0	3.0	1.9	[g]1.1/2.9	[h]0.6	3.0	1.7	9.2	−0.1	38.9	0.35
K52N/H159L	3.7	2.8	1.4	2.7	1.3	[g]0.2/2.5	[h]0.5	3.0	1.2	10.0	1.1	3.2	0.37

[a,b,c]Data from Refs.15 16 and 17, respectively; [d]Units in Kcal/mole; [e]Unit in GuHCl (M.); [f]Units in Kcal/mole/M.; the error estimate for data sets (d to f) was ~± 20%; [g]Two sets of values due to the biphasic nature of the unfolding curve; [h]The value for the second phase because the first phase did not show a plateau value; [i] DNA sequence is lac promoter and units in $x10^{-6}$ M^{-1}; the error estimate was ~± 15%; [j]Fraction of deuterium not exchanged out after one minute; the error estimate was ~± 15%.

significant (Fig. S2). The integration was performed between two valleys of the peak of α-helix (1642 and 1668 cm^{-1}), which was shown as the shaded parts in Fig. S2. This integration procedure is to determine the content of remaining helix at the specific concentration of GuHCl. Under the same conditions, the denaturation of myoglobin was also monitored by intrinsic fluorescence. FT-IR data were nearly identical to the fluorescence data (Fig. S3). It implies that the absorption of GuHCl in the region of interest in FT-IR does not interfere with the area calculation of the peak of α-helix.

In order to test if the FT-IR method can correctly reflect the denaturation behavior of a protein, ribonuclease A, known to unfold with a two-state denaturation mechanism, was used. The unfolding curves of α-helix and β-strand with GuHCl were nearly the same over the transition regions (Fig. S4), an observation consistent with a two-state unfolding process. These two control experiments indicate that FT-IR method is an effective way to monitor the change of the substructures in a protein. In conclusion, FT-IR can reflect the denaturation behavior of a protein induced by GuHCl.

3.3.2. Denaturation of WT CRP

From x-ray crystallography, WT CRP consists of nearly the same content of α-helix as that of β-strand. In the native state, the integrated peak areas of α-helix and β-strand from the second derivative FT-IR spectrum of WT CRP were approximately the same [22], a conclusion that is consistent with the crystallographic data. The peak areas decreased in the unfolding transition regions with increasing GuHCl concentration. However, the decreases were not synchronous for α-helix and β-strands (Fig. 4). The unfolding of α-helix preceded that of β-strands.

The C-helices constitute mainly the subunit-subunit interface of WT CRP. It would be reasonable to expect an unfolding of the C-helices would break the interface leading to dissociation of the dimeric CRP that can be detected by sedimentation equilibrium. The sedimentation equilibrium data from our previous study [15] provide the dimerization constants in native conditions from which we were able to calculate the % dimer at the concentration employed in the spectroscopic studies except those of FT-IR data which were determined at about 12 fold higher concentrations. The results of % dimer were superimposable to the unfolding curve of α-helices as monitored by FT-IR (Fig. 4). Thus, unfolding of helices in WT CRP is apparently tracked by the dissociation of its subunits.

Intrinsic fluorescence data were superimposable to the unfolding curve of β-strands monitored by FT-IR (Fig. 4). Although there was a 12 fold difference in the protein concentration employed by these two methods, the two unfolding curves are essentially identical. It means that β-strands unfolding is highly correlated to the intrinsic fluorescence data. Since the N-terminal cAMP binding domain consists of mainly β-strands, the identity of the unfolding curves monitored by fluorescence and β-strands by FT-IR implies that these two sets of data reflect mostly the stability of the N-terminal domain of CRP.

3.3.3. Denaturation of K52N, H159L and K52N/H159L CRP mutants

Residues 52 and 159 are in two separate domains. Residue 52 resides in the N-terminal cAMP binding domain which is composed mainly of β-strands. Residue 159 resides in the C-terminal DNA binding domain which consists mostly of α-helices. Thus, the stability of α-helices and β-strands approximately represents the stability of the C-terminal and N-terminal domains, respectively. By studying the single mutants of K52N and H159L separately and by monitoring the

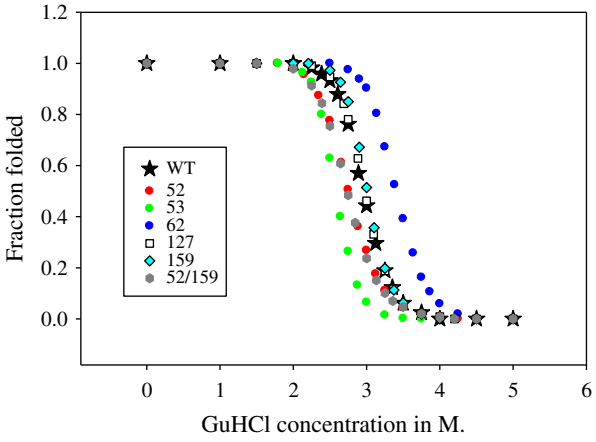

Fig. 3. Chemical denaturation of CRP samples monitored by tryptophan fluorescence. The symbols and identity of CRP samples are the same as in Fig. 2.

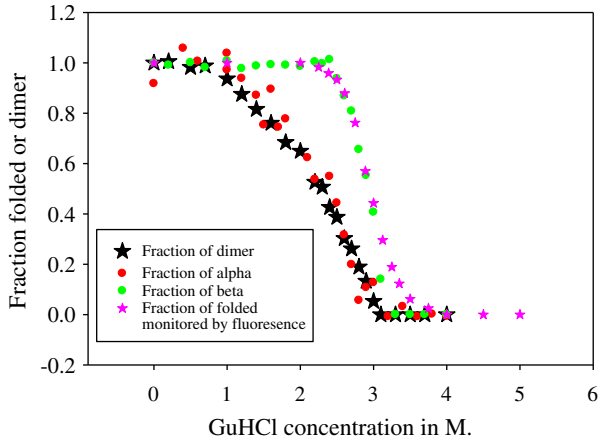

Fig. 4. Fraction of folded and dimer of WT CRP. The symbols and identity of spectroscopic data are: ★, fraction of dimer as determined by sedimentation equilibrium; ●, fraction of folded α-helix as monitored by FT-IR; ●, fraction of folded β-strand as monitored by FT-IR; ★, fraction of folded CRP as monitored by fluorescence.

stability of helices and strands, we expect to deduce the effects of mutations on each domain. The results of the double mutant K52N/H159L are expected to provide information on the communication between domains.

Fig. 5 shows the results of the unfolding curves of K52N CRP monitored by three spectroscopic methods. It is interesting to note that the α-helices unfolded at low GuHCl concentrations while the β-strands seem to be more stable and unfolded at higher GuHCl concentrations. Furthermore, the unfolding curve observed by fluorescence again resembles that of the strands, as in the case for WT CRP. This coincidence of these curves is consistent with the interpretation that the fluorescence data track the unfolding events of the N-terminal cAMP binding domain which consists of mainly β-strands. Contrary to the behavior observed for the WT CRP, the unfolding curve of α-helices does not track the dissociation of subunits. Thus, it seems that the unfolding of helices is not necessarily an event directly linked to subunit dissociation. The α-helices of the K52N mutant apparently were less stable than those of the WT as shown in Fig. 5 and Table 1.

Figs. 6 and 7 summarize the data for the unfolding of the H159L and K52N/H159L double mutants, respectively. The H159L mutation has a very significant destabilizing effect in some of the helices since the unfolding curve is biphasic, indicating the presence of different populations of helices with different stability i.e. ~40% is less stable than the remaining 60%.

The results of the double mutant are even more dramatic since the unfolding curve is not a summation of the curves of the single mutants. 40% of the helices were stabilized significantly; even more so than that of the K52N mutant, while the other 60% exhibited a stability that was between those of the single mutants. The non-additive effects of the double mutant indicate the presence of communications between these two residues, although they reside in different domains.

The unfolding curves of the β-strands of K52N, H159L and K52N/H159L double mutant are apparently similar with minor differences e.g. the K52N mutation seems to destabilize some β-strands in comparison to that of the WT; however, the H159L and double mutant exhibited stabilization of a small percentage of β-strands.

3.3.4. Denaturation of D53H, S62Fand T127L CRP mutants

An equivalent set of experiments were conducted on the D53H, S62F and T127L mutants. Figs. 8 to 10 summarize the unfolding of these mutants. It is interesting to note that, similar to the other mutants, the stability of α-helices was perturbed. D53H differentially destabilized a 40% of helices while the rest seem to retain the same

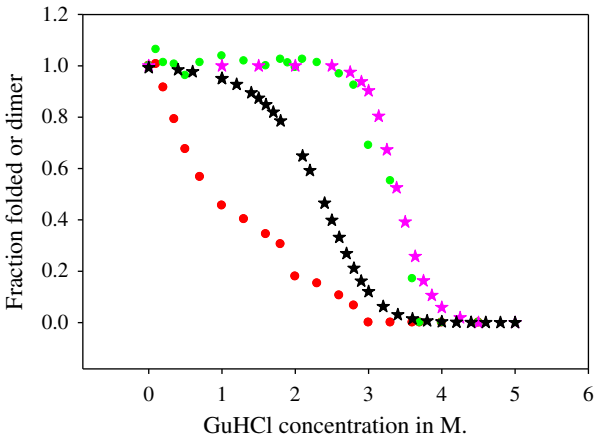

Fig. 6. Fraction of folded and dimer of H159L. The symbols and identity of spectroscopic data are the same as in Fig. 4.

stability of WT CRP, shown in Fig. 8. S62F mutation affected the stability of essentially all the α-helices and the unfolding process did not exhibit the S-shape characteristics of a cooperative process, shown in Fig. 9. The T127L mutation apparently stabilized ~40% of the helices while the stability of the remaining percentage of helices retained the same stability as that of WT CRP, shown in Fig. 10. Unfortunately, these data do not provide any information to establish the identity of these helices, namely, the 40% helices might constitute different helices in each mutant.

The unfolding of the β-strands of the D53H, S62F and T127L mutants showed results similar to those of the other mutants. D53H and T127l mutations seem to shift the strands to lower and higher stability, respectively.

All the parameters for these mutants are summarized in Table 1.

4. Discussion

CRP is emerging as one of the more intensely studied transcription factors for elucidating the basic mechanism of allostery. Both the apo and holo forms of CRP have been defined by NMR spectroscopy and X-ray crystallography [7–9,21,24]. There is consensus in the conclusion derived from NMR and solution thermodynamic studies that protein dynamics plays a significant role in modulating cooperativity of ligand binding [9,14]. One intriguing observation is that CRP can be modulated by mutations to exhibit both positive and negative cooperative in cAMP binding [16,19]. Yet, there are no significant structural changes induced by these mutations [9]. By employing a

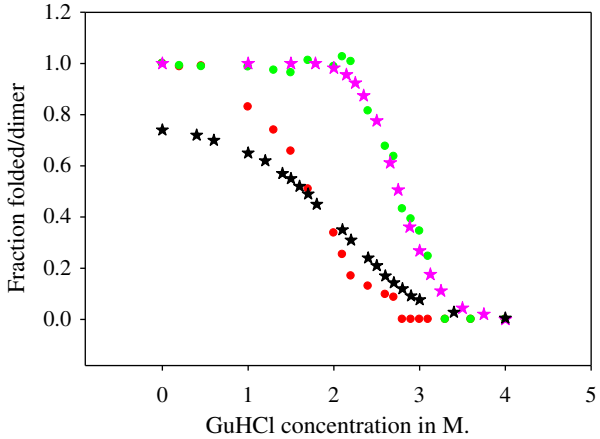

Fig. 5. Fraction of folded and dimer of K52N CRP. The symbols and identity of spectroscopic data are the same as in Fig. 4.

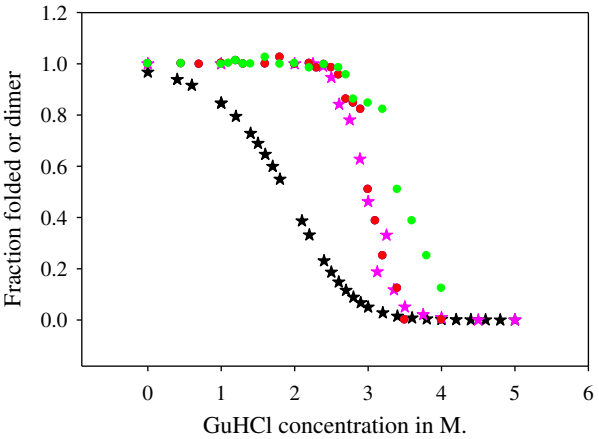

Fig. 7. Fraction of folded and dimer of K52N/H159L CPR. The symbols and identity of spectroscopic data are the same as in Fig. 4.

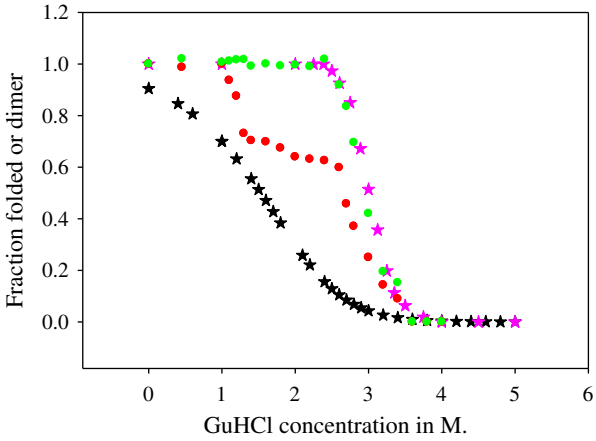

Fig. 8. Fraction of folded and dimer of D53H CRP. The symbols and identity of spectroscopic data are the same as in Fig. 4.

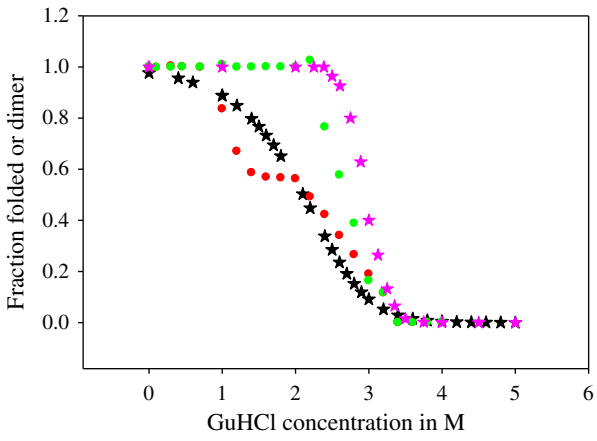

Fig. 10. Fraction of folded and dimer of T1271 CPR. The symbols and identity of spectroscopic data are the same as in Fig. 4.

different approach, we attempted to identify a thermodynamic parameter(s) which could track the perturbations induced by these mutations and as a consequence a change in the allosteric behavior of CRP. We monitored the energetic landscape of CRP through unfolding induced by chemical denaturation using different spectroscopic approaches.

The most significant observation of this study is that mutations can affect the stability of secondary structural elements even though the structures of these mutants are essentially the same in their folded states. Regardless of the location of the residue being mutated, the stability of the α-helices is more significantly perturbed while the perturbation of the β-strands is quite subtle (Figs.4 to 10).

In considering the complete set of data, there are apparently two families of α-helices that are roughly distributed in a ratio of 40:60. Mutation can modulate the stability of these families of helices. Some of the mutations can differentially destabilize a subset of helices so much so that a biphasic unfolding curve can be observed e.g. D53H, S62F, H159L and the double mutant of K52N/H159L. There is no obvious correlation between the stability of the helices with cAMP binding. For example, D53H mutation enhances the positive cooperativity of cAMP while both S62F and H159L mutations lead to negative cooperativity, although in all three cases about 40% of the helices are destabilized (Figs. 6, 8 and 9). At present, there is no information to determine if the same 40% of the helices are destabilized.

Upon closer inspection of the data shown in Figs. 3 to 10, we noticed a pattern of coupling between the α-helices and β-strands as evident in the shifts in their respective unfolding curves. In order to facilitate the comparison in this section of discussion, the data are re-grouped into unfolding curves of secondary structures as shown in Figs. S5A and B and S6A and B (Supplementary Material). Using the unfolding data of WT CRP as the reference state, Figs. S5A and S6A show that the α-helices of T127I and part of that of H159L mutant CRP are more stable than that of WT CRP. The other mutant α-helices are all less stable than that of WT CRP. Figs. S5B and S6B show that the β-sheets of S62F CRP are more stable than that of WT CRP while the β-sheets of the rest of the mutants show either same (T127I, H159L and K52N/H159L) or less stability (D53H and K52N). We use the shifts of the curves as an indication of communications between the α-helices and β-sheets secondary structural elements in these CRP species. Remembering that the cAMP binding domain consists of mainly β-sheets while the DNA binding domain consists of α-helices, we will assume that the unfolding behavior of the cAMP and DNA binding domains are represented by that of the β-sheets and α-helices, respectively. Since the NMR data showed that the S62F mutation decouples the interaction between the cAMP and the DNA binding domain [9], we propose that the unfolding behavior of the β-sheets of S62F CRP represents that of the uncoupled state of the cAMP binding domain. As shown in Fig. S6B, those sheets exhibit the highest stability. As a corollary, we assume that lower stability of β-sheets implies communication between β-sheets and α-helices. Based on this assumption, one may conclude that there is communication between the two classes of secondary structures in all the other CRP species since their unfolding curves have all shifted in comparison with that of the S62F mutant. Hence, one may conclude that the mutations are affecting the communications between the domains and the consequence of the change in communication is reflected in the stability of the secondary structures.

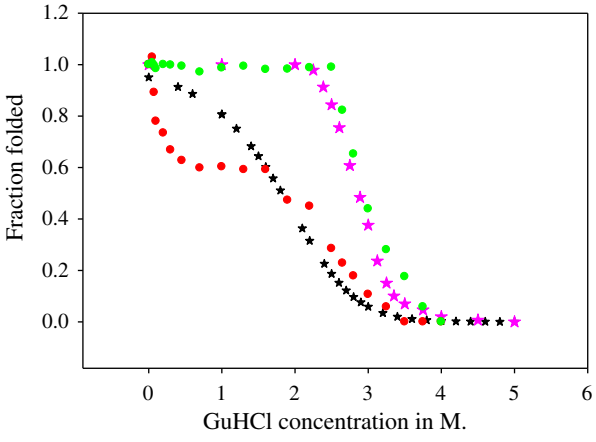

Fig. 9. Fraction of folded and dimer of S62F CRP. The symbols and identity of spectroscopic data are the same as in Fig. 4.

The apparent lack of correlation between ΔG of stability with ΔG of cAMP binding or ΔΔG of binding of the 1st and 2nd molecule of cAMP may mean that other thermodynamic parameter such as entropy might be the factor that is important in modulating allostery. Such a speculation is consistent with the NMR study [9] which concluded that structural entropy plays an important role in allostery. Our published H/D exchange data [14] established a linear correlation between global protein dynamics and magnitude of cooperativity. The less dynamic protein exhibits a lower affinity for the 2nd cAMP molecule.

The tracking of structural energetics of the helices and DNA binding is less clear. The DNA binding site is located in the C-terminal domain of CRP which consists of mainly α-helices. The mutations that lead to lower affinity for DNA include K52N, S62F, T127L and the K52N/H159L double mutant. However, K52N and T127L induce lower and higher stability, respectively. The S62F mutation destabilizes all the helices significantly while the K52N/H159L double mutant

induces a differential effect on the stability on the various helices i.e. destabilize some helices but stabilizes others in the same molecule. A really interesting observation for the D53H mutation is that the mutation enhances the binding affinity of the 2nd cAMP and DNA drastically. Yet, ~40% of helix is destabilized while the remaining ~60% is stabilized, a pattern similar to that of K52N/H159L double mutant which shows an opposite functional properties in comparison with the D53H mutation. Hence, there is no clear pattern in the stability of the helices to correlate to DNA and cAMP binding. This study demonstrates that the stability of the α-helices of CRP is more susceptible to mutations regardless of the location of the mutation site while the β-strands are more stable and the perturbations are more subtle in magnitude.

In summary, the nature of the cooperative binding of cAMP is probably modulated by the entropy of stability of secondary structures of CRP. Too rigid a CRP may diminish the ability to adopt a conformation of CRP that binds the 2nd cAMP more favorably. At present, since the techniques we employed do not enable us to identify the specific helices that are stabilized or destabilized, a more focused study is being pursued to elucidate the effects of perturbation in enthalpy and entropy one residue at a time.

5. Dedication

This manuscript is dedicated to the celebration of the 25th anniversary of the Gibbs Conference on Biological Thermodynamics, a conference that provides many of the knowledge and encouragement without which this work might not have been done. JCL dedicates this work to the memory of Gary K. Ackers who was the major driving force in establishing the Gibbs Conference which continues to be the learning center of biological thermodynamics for new generations of biological scientists.

Acknowledgement

Supported by NIH Grants GM-45579 and GM-77551 and the Robert A. Welch Foundation.

Appendix A. Supplementary data

Supplementary data to this article can be found online at doi:10.1016/j.bpc.2011.06.015.

References

[1] S. Adhya, S. Garges, Positive control, J. Biol. Chem. 265 (1990) 10797–10800.
[2] S. Busby, H. Buc, Positive regulation of gene expression by cyclic AMP and its receptor proteinin Escherichia coli, Microbiol. Sci. 4 (1987) 371–375.
[3] B. de Crombrugghe, S. Busby, H. Buc, H. Cyclic, AMP receptor protein: role in transcription activation, Science 224 (1984) 831–838.
[4] W.S. Reznikoff, Catabolite gene activator protein activation of lac transcription, J. Bacteriol. 174 (1992) 655–658.
[5] H. Aiba, S. Fujimoto, N. Ozaki, Molecular cloning and nucleotide sequencing of the gene for E. coli cAMP receptor protein, Nucleic Acids Res. 10 (1982) 1345–1361.
[6] P. Cossart, B. Gicquel-Sanzey, Cloning and sequencing of the crp gene of Escherichia coli K12, Nucleic Acids Res. 10 (1982) 1363–1378.
[7] H. Sharma, S. Yu, J. Kong, J. Wang, T.A. Steitz, Structure of apo-CAP reveals that large conformational changes are necessary for DNA binding, Proc. Natl. Acad. Sci. U. S. A. 106 (2009) 16604–16609.
[8] S.-R. Tzeng, C.G. Kalodimos, Dynamic activation of an allosteric regulatory protein, Nature 462 (2009) 368–372.
[9] N. Popovych, S.-R. Tzeng, M. Tonelli, R.H. Ebright, C.G. Kalodimos, Structural basis for cAMP-mediated allosteric control of the catabolite activator protein, Proc. Natl. Acad. Sci. U. S. A 106 (2009) 6927–6932.
[10] X.D. Cheng, J.C. Lee, Interactive and Dominant Effects of Residues 128 and 141 on Cyclic Nucleotide and DNA Bindings in *E.coli* cAMP Receptor Protein, J. Biol. Chem. 273 (1998) 705–713.
[11] J.M. Passner, S.C. Schultz, T.A. Steitz, Modeling the cAMP-induced allosteric transition using the crystal structure of CAP-cAMP at 2.1 A resolution, J. Mol. Biol. 304 (2000) 847–859.
[12] S. Garges, S. Adhya, Sites o f Allosteric Shift in the Structure of the Cyclic AMP Receptor Protein, Cell 41 (1985) 745–775.
[13] J.G. Harman, Allosteric regulation of the cAMP receptor protein, Biochim. Biophys. Acta 1547 (2001) 1–17.
[14] K. Gekko, N. Obu, J. Li, J.C. Lee, A Linear Correlation Between the Energetics of Allosteric Communication and Protein Flexibility in E. coli Cyclic AMP Receptor Protein Revealed by Mutation-Induced Changes in Compressibility and Amide Hydrogen/Deuterium Exchange, Biochemistry 43 (2004) 3844–3852.
[15] S.H. Lin, L. Kovac, A.J. Chin, C.C.-Q. Chin, J.C. Lee, Ability of *E.coli* Cyclic AMP Receptor Protein to Differentiate Cyclic Nucleotides: Effects of Single Site Mutations, Biochemistry 41 (2002) 2946–2955.
[16] S.H. Lin, J.C. Lee, Communications Between the High Affinity Cyclic Nucleotide Binding Sites in *E.coli* Cyclic AMP Receptor Protein: Effect of Single Site Mutations, Biochemistry 41 (2002) 11857–11867.
[17] S.H. Lin, J.C. Lee, Linkage of Multiequilibria in DNA Recognition by the D53H *E.coli* cAMP Receptor Protein, Biochemistry 41 (2002) 14935–14943.
[18] S. Yu, J.C. Lee, Role of Residue 138 in the Inter-domain Hinge Region in Transmitting Allosteric Signals for DNA Binding in E. coli cAMP Receptor Protein, Biochemistry 43 (2004) 4662–4669.
[19] J. Dai, S.H. Lin, C. Kemmis, A. Chin, J.C. Lee, Interplay between Site-specific Mutations and Cyclic Nucleotides in Modulating DNA Recognition by E. coli Cyclic AMP Receptor Protein, Biochemistry 43 (2004) 8901–8910.
[20] E.J. Lee, J. Glasgow, S.F. Leu, A.O. Belduz, J.G. Harman, Mutagenesis of the cyclic AMP receptor protein of Escherichia coli: targeting positions 83, 127 and 128 of the cyclic nucleotide binding pocket, Nucleic Acids Res. 22 (1994) 2894–2901.
[21] X.D. Cheng, M.L. Gonzalez, J.C. Lee, Energetics of Intersubunit and Intrasubunit Interactions of E.coli cAMP Receptor Protein, Biochemistry 32 (1993) 8130–8139.
[22] A. Dong, J.M. Malecki, L. Lee, J.F. Carpenter, J.C. Lee, Ligand-induced Conformational and Structural Dynamic Changes in *E.coli* Cyclic AMP Receptor Protein, Biochemistry 41 (2002) 6660–6667.
[23] A. Polit, U. Błaszczyk, Z. Wasylewski, Steady-state and time-resolved fluorescence studies of conformational changes induced by cyclic AMP and DNA binding to cyclic AMP receptor protein from Escherichia coli, Eur. J. Biochem. 270 (2003) 1413–1423.
[24] I.T. Weber, T.A. Steitz, Structure of a Complex of Catabolite Gene Activator Protein and Cyclic AMP Refined at 2–5 A Resolution I, J. Mol. Biol. 198 (1987) 311–326.